

Erik J. Kobylarz, Andrew E. Hudson, Ayeesha Kamal, Robert J. DeBellis, Nicholas D. Schiff
 Department of Neurology and Neuroscience, Weill Medical College of Cornell University, 1300 York Ave, New York, New York, 10021 USA

INTRODUCTION

The minimally conscious state (MCS) is characterized by reliable but inconsistent behavioral evidence of self or environmental awareness. MCS patients demonstrate one or more fluctuating but reproducible behaviors, such as following simple commands, producing yes/no responses or intelligible verbalization or gestures. Patients may evolve to MCS from coma or the vegetative state after severe head injury or other types of brain injury. This distinction is important for determining prognosis, treatment decisions and medico-legal judgments. Some studies show evidence for a high rate of misdiagnoses among orders of consciousness (Giaccio, et al. 2002). The prevalence of MCS is estimated to be 112,000-280,000 adult and pediatric patients in the U.S. (Strauss et al. 2000).

Power spectrum and coherence analyses of the electroencephalogram (EEG) have often been used to study brain dysfunction. Such quantitative analyses can be of prognostic significance. More favorable outcome from traumatic coma has been correlated with higher alpha and beta band power over the left hemisphere, particularly fronto-centrally and centro-temporally. Coherence, a measure of cross-correlation in the frequency domain, implies changes in functional connectivity, which can be more useful than power in assessing functional integrity in setting of brain injury (Davey et al. 2000).

We employed power spectral and coherence analyses of the EEG in the awake and asleep states in order to study potential underlying mechanisms of the minimally conscious state.

METHODS

Subjects and experimental conditions: We recorded continuous EEG using the standard 10-20 electrode placement system from two patients in the MCS for more than 18 months following severe brain injury. Both patients suffered a unilateral cortical and sub-cortical brain damage with relative preservation of the contralateral hemisphere. Functional brain imaging in both patients revealed widely recruitable large-scale networks (Schiff et al. 2005).

Patient 1 is a 33 year old right-handed man who sustained a closed head injury during an assault 24 months prior to this study. Initial blunt trauma to the right frontal region produced bilateral subdural hematomas that resulted in a central herniation syndrome prior to their surgical evacuation. At the time of this study, the patient remained in active rehabilitation throughout the two-year period following the initial injury with repeated achievement of treatment milestones and subsequent regression of gains ("cognitive impersistence"). At the time of this study the patient was alert and occasionally produced verbal output. Neurological exam revealed that he had intact visual saccades to stimuli and could inconsistently follow complex behavioral tasks (eg. no-go with verbal cues and countermanding). His performance, however, was inconsistent even within one examination period. Visual pursuit was intact, with some restriction of movement toward the left visual field. The right pupil was minimally reactive at 2 mm and the left pupil was fixed at 3 mm. The ocular reflex for smooth pursuit was released and oculomotor response despite being able to follow commands and to voluntarily saccade. Optokinetic responses were present for horizontal, but not vertical gaze. Motor exam was notable for marked weakness in muscles of all four extremities, a fine tremor of the left upper extremity, and a left "vertical thumb" sign. Axial tone was also increased. The patient was able to localize external stimuli. Pathological reflexes included a glabellar reflex that extinguished, a right palmo-mental sign and bilateral grasp reflexes.

Patient 2 is a 21 year old right-handed man who suffered a spontaneous left temporal-parietal hemorrhage. His initial exam demonstrated extensor posturing to noxious stimuli with occasional flexion responses. Initial CT scans showed a large left intracerebral hemorrhage with midline shift and mass effect, which produced transtentorial herniation. The hemorrhage was evacuated within 24 hours. More than one year after injury, the neurological exam revealed alert-appearing wakefulness, and a preserved ability to track and saccade to stimuli. Using the left arm the patient was able to inconsistently move to command and respond to yes/no questions. During the course of inpatient evaluations for this study the patient was noted to elicit a wrist-wag with the intelligible verbalization: "Mouthpiece of words was first noted 11 months after initial injury. He experienced recurrent diaphoretic crises and crying outbursts, but has also been noted to demonstrate contingent emotional responses (first noted 5 months post-injury). At his best level of function he would follow one step routine commands which then decayed (e.g. open eyes, close eyes). The family reported that, at his best, he demonstrated an intermittently able to name family members (single words).

Power spectra and coherence functions were computed from artifact-free EEG segments recorded during sleep and wakefulness using multi-taper methods of spectral analysis.

Data analysis: EEG signals were reviewed and data recorded from electrodes without significant artifact were analyzed. This resulted in the removal of the EEG data from the temporal leads for Patient 2. Artifact-free data during wakefulness and sleep were selected, and data were grouped together by condition. We examined power spectra at frequencies ranging from 0 to 100 Hz from each EEG channel (displayed up to 50 Hz on this poster). We computed coherence spectra for each of the leads with their nearest intrahemispheric neighbors.

Power spectra summarize the frequency content of the time-varying EEG signal and index the relative strength of contribution of particular frequencies to the overall composite signal.

The coherence of two signals provides a measure of cross-correlation in the frequency domain and can be thought of as an index of dynamic interaction of two signals as a function of frequency (Bendat and Piersol, 2000). The coherence is computed from the cross spectrum at a given frequency f normalized by the power spectra of each signal (using the square root of the sum of their squares, see Eq. 6 below). This obtaining peaks or troughs in the coherence is not simply the result of a strong local maximum or minimum within a frequency range of one or the other power spectrum (e.g., see Results panel for Patient 1, F4, T4, C4 coherence).

Power and coherence spectra were computed using multi-taper methods (Thomson and Chave 1991, Mitra and Pesaran 1999) on 3 second (for awake state) or 5 second (for asleep state) swatches of data sampled at 200 Hz. Three Slepian data tapers were used for the power spectra and coherence spectra to obtain a frequency resolution of 1/3 Hz. The multi-taper method is based on the use of multiple orthogonal data tapers to stabilize the variance and optimize the bias of a spectral estimate. A direct estimate of the power spectrum, $S_{xx}(f) = \frac{1}{T} | \int_{-T/2}^{T/2} x(t) e^{-j2\pi ft} dt |^2$, is calculated using this method by averaging over individual tapered spectral estimates:

$$\hat{S}_{xx}(f) = \frac{1}{K} \sum_{k=1}^K | \int_{-T/2}^{T/2} x(t) e^{-j2\pi ft} dt |^2$$

The weights w represent the sequence of orthogonal data tapers, w is the signal. The estimate of the power spectrum is obtained by averaging over the tapered estimates:

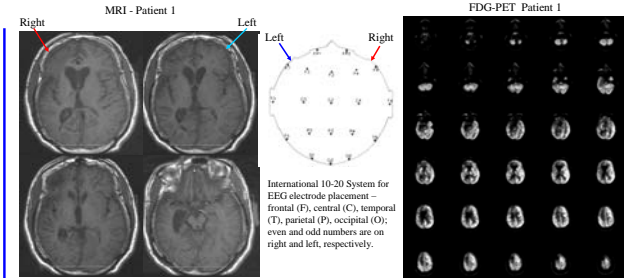
$$\hat{S}_{xx}(f) = \frac{1}{K} \sum_{k=1}^K | \int_{-T/2}^{T/2} x(t) e^{-j2\pi ft} dt |^2$$

The coherence spectrum, $C_{xy}(f)$, is similarly obtained from multi-taper estimates of the power spectra from two signals ($S1$ and $S2$, see Eq. 6 below). To calculate confidence limits for our spectra we use jackknife methods as developed by Thomson and Chave (1991). The logarithm of the power spectrum at a single frequency is used to stabilize the estimation procedure. Delete-one jackknife estimates are formed in (3) and their average (4) to obtain a spectrum estimate. The jackknife estimate of the variance of the log power spectrum is given by (5). Using these quantities it is possible to construct confidence intervals for the power spectra and coherence estimates shown on the poster (see Thomson and Chave 1991). Coherence estimates at a frequency f are computed as shown in Eq. 6.

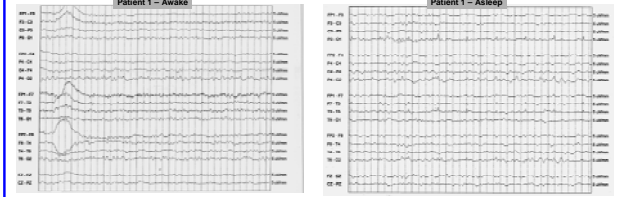
$$\ln \hat{S}_x = \ln \left[\frac{1}{N} \sum_{n=1}^N \hat{S}_x^n \right]$$

$$\sigma^2 = \text{var}(\ln \hat{S}_x) = \frac{N-1}{N} \sum_{n=1}^N (\ln \hat{S}_x^n - \ln \hat{S}_x)^2$$

$$\hat{C}_{xy}(f) = \frac{\sum_{n=1}^N \hat{S}_x^n \hat{S}_y^n}{\sqrt{\sum_{n=1}^N \hat{S}_x^n} \sqrt{\sum_{n=1}^N \hat{S}_y^n}}$$



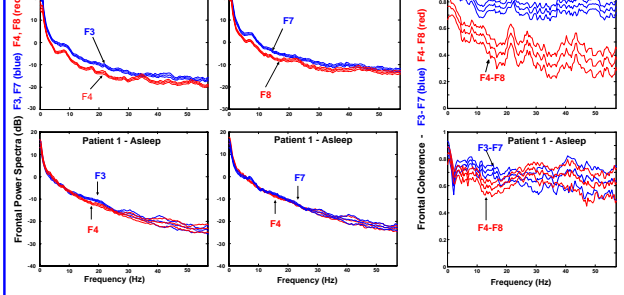
Structural MRI from Patient 1 reveals right frontal lobe encephalomalacia and an old right thalamic infarct in the paramedian region.



FDG-PET studies for Patient 1 demonstrated marked reduction of right hemispheric metabolism, notably in the frontal and thalamic regions.

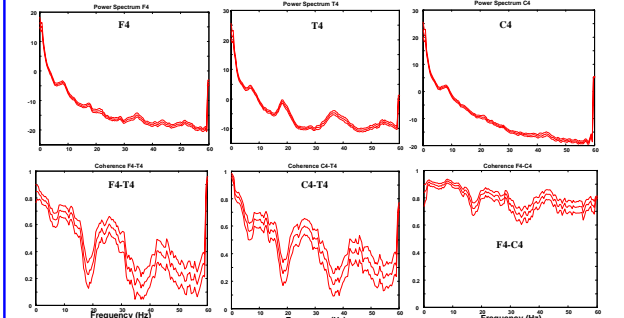
Awake EEG segment from Patient 1 revealing a disorganized background with a 5-6 Hz posterior dominant rhythm, more apparent in the right hemisphere, and a predominance of beta activity in the left. Continuous polymorphic slowing was observed bilaterally, more prominently over the right hemisphere.

Asleep EEG segment from Patient 1 shows slowing and diminished sleep spindles on the right more than the left.

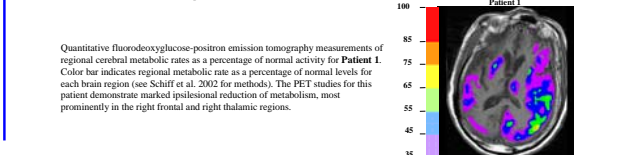


For both patients the power spectra revealed generally few significant differences between corresponding hemispheric regions but sharp reductions in interregional coherence over the damaged hemisphere that correlates with the reduced thalamic metabolism in both patients.

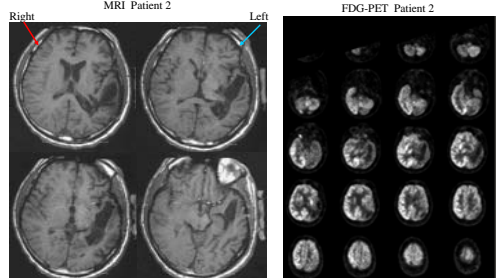
Power Spectra and Coherence Spectra F4, T4, C4 – Patient 1 Awake



Throughout the right hemisphere in Patient 1 awake eye-closed data we identify dips in the coherence across electrode pairs at 18 Hz and higher harmonics. For some of the individual channel spectra peaks at 18 Hz and higher harmonics are identified. The dips in the coherence are due to the contribution of the denominator and not the cross spectrum numerator (data not shown). These findings indicate that although excess power at these frequencies is present in more than one channel the sources act as independent noises and are uncorrelated.



Quantitative fluorodeoxyglucose-positron emission tomography measurements of regional cerebral metabolic rates as a percentage of normal activity for Patient 1. Color bar indicates regional metabolic rate as a percentage of normal levels for each brain region (see Schiff et al. 2002 for methods). The PET studies for this patient demonstrated marked ipsilateral reduction of metabolism, most prominently in the left frontal and right thalamic regions.



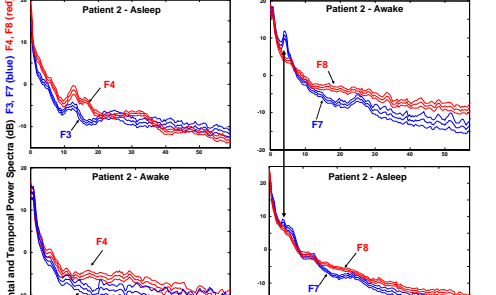
Structural MRI imaging from Patient 2 demonstrating a large area of encephalomalacia over the left temporal-parietal region with dilatation of the left lateral ventricle, particularly surrounding the temporal and occipital horns.



FDG-PET study from Patient 2 demonstrated marked reduction of left hemispheric metabolism, notably in the temporal, parietal and thalamic regions.

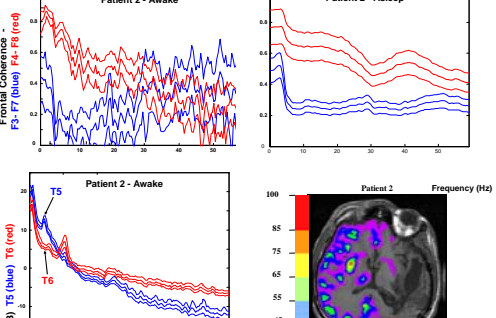
Awake EEG segment from Patient 2 revealing a 9-10 Hz posterior dominant rhythm and mildly disorganized background with a 5-6 Hz posterior dominant rhythm, more apparent in the right hemisphere, and a predominance of beta activity in the left hemisphere, most apparent fronto-temporally, and occasional isolated sharp waves in the posterior left hemisphere.

Asleep EEG segment from Patient 2 shows continuous moderate left central and posterior polymorphic slowing. Sleep spindles are present bilaterally, on the right greater than the left.

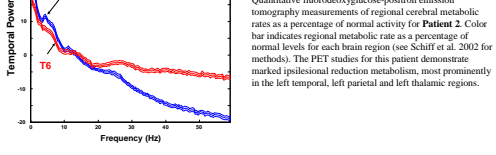


For both patients the power spectra revealed generally few significant differences between corresponding hemispheric regions but sharp reductions in interregional coherence over the damaged hemisphere that correlates with the reduced thalamic metabolism in both patients.

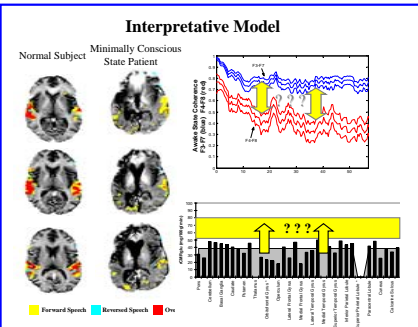
Power Spectra and Coherence Spectra F4, T4, C4 – Patient 2 Awake



Throughout the right hemisphere in Patient 1 awake eye-closed data we identify dips in the coherence across electrode pairs at 18 Hz and higher harmonics. For some of the individual channel spectra peaks at 18 Hz and higher harmonics are identified. The dips in the coherence are due to the contribution of the denominator and not the cross spectrum numerator (data not shown). These findings indicate that although excess power at these frequencies is present in more than one channel the sources act as independent noises and are uncorrelated.



Quantitative fluorodeoxyglucose-positron emission tomography measurements of regional cerebral metabolic rates as a percentage of normal activity for Patient 2. Color bar indicates regional metabolic rate as a percentage of normal levels for each brain region (see Schiff et al. 2002 for methods). The PET studies for this patient demonstrate marked ipsilateral reduction of metabolism, most prominently in the left temporal, left parietal and left thalamic regions.



Interpretative Model

In both MCS patients studied here we were able to correlate the quantitative EEG measurements and FDG-PET findings with MRI studies that demonstrate preserved large-scale network activations in response to language and somatosensory stimuli (see Schiff et al. 2005; image above is from Patient 1 on poster). Both patients demonstrated low global resting metabolic rates (as seen in the single co-registered MRI-PET images shown here) with significant differences in hemispheric and thalamic resting metabolic rates. As shown on the poster, the resting awake EEG studies in both patients reveal significant reductions in inter-regional coherence of the more damaged hemisphere. These abnormalities of EEG coherence indicate a significant alteration of the functional integration of cortical regions in the more damaged hemisphere. For Patient 1, this interregional coherence pattern has a marked dependence on arousal state with coherence decreases observed across frequencies only in the state of wakefulness.

In context of the low resting metabolic activity seen for both patients, the preservation of large-scale network responses suggest a potential cerebral reserve that is dormant but potentially functional networks that remain inactive due to globally reduced neuronal activity. The quantitative EEG findings suggest that the abnormalities observed in the coherence measurements obtained during wakefulness could be a possible marker of abnormal dynamics masking greater network response. Salient stimuli such as personally meaningful narratives (Schiff et al. 2005, see adjacent poster #334.21) may produce changes in both resting metabolism and interregional EEG coherence as suggested by the yellow arrows shown on the coherence spectra and FDG-PET data obtained from the patient in a resting wakeful state. The findings support developing longitudinal assessments of the evolving EEG in patients with severe brain injury.

CONCLUSIONS

1. The striking finding of a sharp reduction of EEG coherence across inter-regional electrode pairs of one hemisphere correlates with ipsilateral thalamic hypometabolism in both patients.
2. These findings are similar to earlier studies of a unique vegetative state patient with severe asymmetric brain damage with total loss of the right thalamus who demonstrated marked reduction in ipsilateral EEG coherence without significant hemispheric differences in the power spectrum (Davey et al. 2000).
3. In one patient we observe that such marked differences in EEG coherence can be state-dependent, with more apparent reduction over wider frequency ranges during wakefulness than during sleep.
4. A possible anatomical and physiological basis for this selective change in EEG coherence is damage to paramedian mesencephalic structures which mediate communication between cortical areas. These structures are damaged during transtentorial herniation (an element in the clinical history of both patients studied here).
5. Thalamic hypometabolism on the side of decreased coherence supports the possible role of disfacilitation producing the hemispheric coherence abnormalities due to a withdrawal of common thalamic excitatory inputs to the cerebral cortex.
6. The finding of an ipsilateral feature of peaks in the power spectrum at 18 Hz and higher harmonics with dips in the coherence spectrum suggests a specific dynamic disturbance during the awake state for Patient 1 originating in the beta frequency range.
7. Taken together with the FDG-PET findings of severe metabolic depression in resting (awake) states, the EEG findings suggest a possible basis for the dissociation of low metabolism despite MRI evidence in both patients of integrative network responses that organize both hemispheres (Schiff, et al. 2005). The dissociation of resting interregional coherence in the left and right hemispheres may thus index differences in the baseline functional integration in MCS patients that are partially reversible.
8. These findings further suggest the utility of using passive stimulation paradigms to assess potential within state changes in EEG power spectra and coherence (see next poster, Goldfine et al. 2005 #334.21).

ACKNOWLEDGEMENTS

We thank Dr. Partha Mitra and MBL Neuroinformatics course for signal processing consultation. Dr. Diana Moreno and Dr. Bradley Beattie for expert assistance with FDG-PET data processing. We thank Sudhin Thomas for expert assistance with data analysis and poster production. These studies were supported by The Charles A. Dana Foundation, NIH-NINDS (NS45451), and WMC GCRC M01 RR00047

REFERENCES

Bendat, J.S., Piersol, A.G. (2000) Random data. J Wiley Interscience
 Cronin NE, Boatman D, Gordon B, Hao L, (2001) Induced electroencephalographic gamma activity during auditory perception. *Clin Neurophysiol.* 112(4):565-82.
 Davey MP, Victor JD, Schiff ND. Power spectra and coherence in the EEG of a vegetative patient with severe asymmetric brain damage. *Clin Neurophysiol* 2000;111:1949-1954
 Giaccio, J.T., Ashwal, S., Chalkin, N., Crawford, R., Jennett, B., Katz, D.L., Kelly, J.P., Rosenberg, J.H., Whyte, J., Zafonte, R.D., Zasler, N.D., (2002) The minimally conscious state: definition and diagnostic criteria. *Neurology* 58, 349-53.
 Kobylarz, E., and Schiff, N.D. (2004) Functional imaging of severely brain injured patients: progress, challenges, and limitations. *Archives of Neurology* 61(9):1357-6.
 Lammni MH, Smith WS, Tate RL, Taylor CM. (2005) The minimally conscious state and recovery potential: a follow-up study 2 to 5 years after traumatic brain injury. *Arch Phys Med Rehabil* 86(4):746-54.
 Mitra P.P., Pesaran, B. (1999) Analysis of dynamic brain imaging data. *Biophysical Journal* 76(2):691-708
 Schiff, N., Ribary, U., Muzum, D., Beattie, B., Kronberg, E., Blaberg, R., Giaccio, J., McCagg, C., Fins, J.L., Llinas, R., and Ploren, F. (2002a). Residual cerebral activity and behavioral fragments in the persistent vegetative state. *Brain* 125, 1210-1234.
 Schiff, N., Rodriguez-Moreno, D., Kamal, A., Petrovich, N., Giaccio, J., Plum, F. and Hirsch, J. (2005) fMRI reveals large-scale network activation in minimally conscious patients. *Neurology* 64(5):523-523
 Schiff, N.D. (2005) Modeling the minimally conscious state: measurements of brain function and therapeutic possibilities. *Progress in Brain Research* 150:477-497
 Strauss DJ, Ashwal S, Day SM, Shavelle RM (2000) Life expectancy of children in vegetative and minimally conscious states *Pediatr Neuro* 23(4):312-9
 Thomson, D.J. (1982) Spectrum estimation and harmonic analysis. *Proceedings of the IEEE*, 70: 1055-96.
 Thomson, D.J. and Chave, A.D. (1991) Jackknife error estimates for spectra, coherences and transfer functions. In: *Advances in Spectrum Analysis and Array Processing* Vol 1. Ed. Haykin, S. Prentice Hall, Englewood Cliffs, NJ, pp. 58-115